Biocatalysis and Agricultural Biotechnology 17 (2019) 427–440

Contents lists available at ScienceDirect

Biocatalysis and Agricultural Biotechnology

journal homepage: www.elsevier.com/locate/bab

Conceptual design of hybrid PCSK9 lead inhibitors against coronary artery disease

Ayarivan Puratchikody[a,*], Navabshan Irfan[a,b], Sakthivel Balasubramaniyan[a]

[a] Drug Discovery and Development Research Group, Department of Pharmaceutical Technology, BIT campus, Anna University, Tiruchirappalli 620 024, India
[b] Crescent School of Pharmacy, B.S.Abdur Rahman Crescent Institute of Science & Technology, GST Road, Vandalur, Chennai 600 048 Tamilnadu, India

ARTICLE INFO

Keywords:
Coronary Artery Disease
PCSK9 inhibitors
Novel ligand generation
Structure based pharmacophore
Ludi
BREED algorithm

ABSTRACT

The enzyme, Proprotein Convertase Subtilisin Kexin type-9 (PCSK 9) inhibition serves as a significant target to prevent the risk of Coronary Artery Disease. Hence, this work is focused on the exploration of novel PCSK 9 lead inhibitors through *In silico* approach. In abidance to the study, BREED algorithm has been taken to design novel hybridised ligands. Subsequently, various *in silico* screening studies were performed in Biovia Discovery Studio 2017. Novel ligand generation protocol generated 595 hybridised ligands from the 51 parent scaffolds. These ligands were mapped and screened by ludi interactions of the active site PCSK 9 and were reduced to 245 hit compounds. The docking studies showed that the berberine skeleton contained molecule possessed CDOCKER energy (−13.5582 Kcal/mol) and formed strong interactions with Arg^{93}, Arg^{97} and His^{137} residues. The developed pharmacophore model revealed that hydrogen bond acceptor and negative ionizable charges are necessary for the inhibition of PCSK 9. The mapping of pharmacophore model confirmed that 96 molecules were as best fit. Finally, toxicity and dynamic simulation studies confirmed that safe and stable complex formation between lead molecules and PCSK 9 receptor. The results concluded that the 15 lead molecules are proved as potent and safe PCSK9 inhibitors.

1. Introduction

Coronary artery disease (CAD) Ischemic heart disease has been the leading cause of death worldwide for the past one and a half decade (WHO, 2018a, 2018b; Rao et al., 2015). The current scenario of heart disease in India is startling that, by the year 2020, the burden of cardiovascular diseases in India will transcend that of any other country in the world (WHO, 2015). CAD deaths in India during 1990 were 10.1 million, and by 2020, the death rate would be 22.1 million, an increase of 119% (Krishnan, 2012). Coronary artery disease is the accumulation of fat on the walls of the artery that supplies blood to the heart. Due to the plaque deposits, the coronary artery is either narrowed or blocked, causing reduced oxygen rich blood supply to the heart, thereby leading to coronary artery disease and various other cardio vascular diseases (Willerson and Holmes, 2004; Mendis et al., 2011). There are various risk factors for CAD, with hypercholesterolemia, i.e. elevated bad cholesterol or low-density lipoprotein (LDL) cholesterol being one of the major modifiable risk factors. Hypercholesterolemia can be treated by a number of cholesterol medications, among which statins being the most potent traditional cholesterol lowering drugs. However, it is associated with various side effects like myalgia, memory loss, type 2 diabetes etc., demanding the development of novel cholesterol lowering medications (Rallidis and Lekakis, 2016; Maji et al., 2013)

In recent years, a newer class of cholesterol lowering enzyme, Proprotein Convertase Subtilisin Kexin type-9(PCSK9) inhibitors have gained researchers attention. The LDL binds to the LDL-receptor leading to the metabolism of LDL, and simultaneously the LDL receptors are recycled back to the surface of the liver. But PCSK-9 binds to the LDL receptors and degrades them. As a result, the LDL receptors cannot be recycled back leading to the elevated LDL level. Hence, by inhibiting PCSK9, a number of LDL receptors are available on the surface of the liver thereby alleviating blood cholesterol level (Farnier, 2014; Steinberg and Witztum, 2009). From the literature search, it is known that there are no existing small molecules against PCSK9 (Momtazi et al., 2017), and the only available PCSK-9 inhibitors are monoclonal antibodies such as Alirocumab and Evolocumab (Sabatine et al., 2017; Natarajan and Kathiresan, 2016), which can cause severe infection at the site of injection and various side effects even leading to the termination of the treatment (Robinson et al., 2015). Further, development of another such monoclonal antibody Bococizumab was discontinued due to a high level of immunogenicity and injection site reactions. In consideration with the limitations with the existing cholesterol

* Corresponding author.
E-mail address: puratchipharma@gmail.com (A. Puratchikody).

https://doi.org/10.1016/j.bcab.2018.12.014
Received 1 October 2018; Received in revised form 7 November 2018; Accepted 11 December 2018
Available online 17 December 2018
1878-8181/

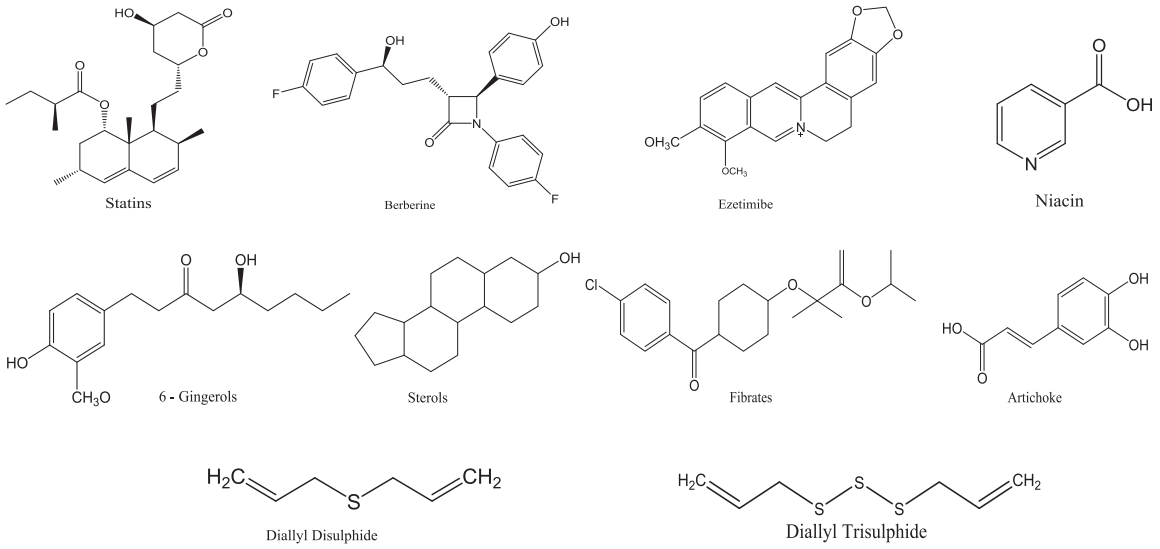

Fig. 1. Basic skeletons of 10 classes of cholesterol lowering compounds.

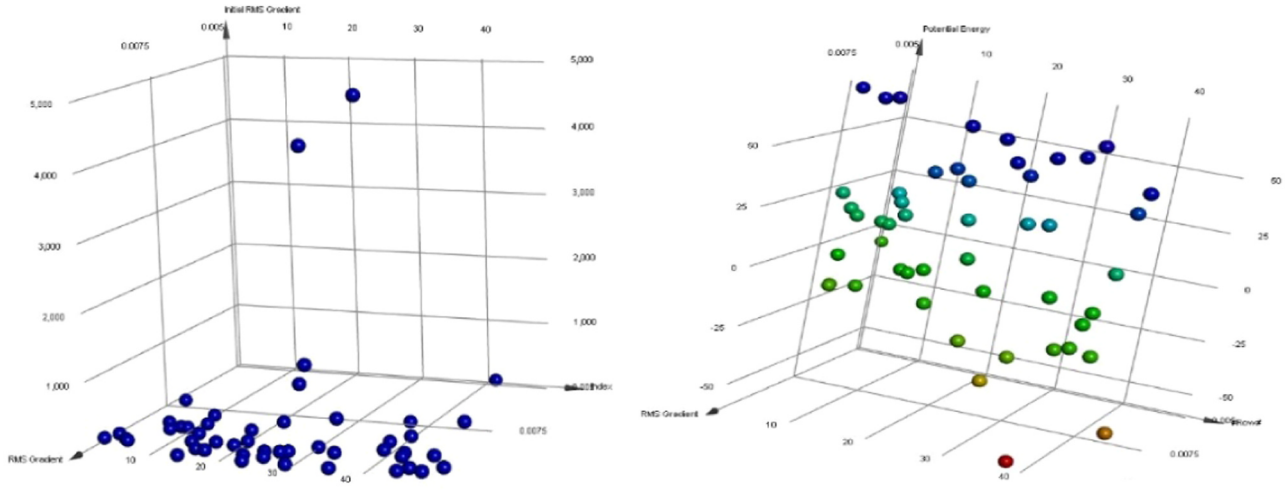

Fig. 2. Potential energy and RMS gradient reduction using smart minimiser algorithm.

medications, there is an increasing exigency to develop novel drugs with high efficiency but low toxicity.

Computer aided drug design is a useful tool to identify a suitable binding site in the target and develop drugs based on the binding site, thus eliminating the chemical molecules that are not promising or has toxicity in the very early stages of drug development. In this study, various computational methodologies were used to identify potent ligands for the target PCSK9, and the results from various studies showed that the identified novel ligands could be potential drugs to treat hypercholesterolemia and thereby prevent the risk of coronary artery disease. It has also been found that the identified lead PCSK9 inhibitors has not been reported yet and are undeniably novel.

2. Methodology

The research findings and all the *in silico* studies of novel PCSK9 inhibitors were investigated in the Biovia Discovery Studio 2017 software (DS).

2.1. Preparation of ligand database

The phytoconstituent and some of the synthetic compounds were collected from the literature based on the cholesterol reducing profiles (Rubins et al., 1999; Ried, 2016; Khera et al., 2015; Wongbutdee, 2009; Li et al., 2015; Singh and Mahajan, 2013). Chiefly, Natural compounds such as berberine, niacin (Farmer, 2009), gingerol, artichoke, allicin, diallyl disulphide, diallyl trisulphide compounds (Corzomartinez et al., 2007) and synthetic compounds such as statins, fibrates, sterols (Abumweis et al., 2008) and ezetimibe (Fig. 1) were selected as parent skeletons to develop new ligands. A total of 51 compounds were identified for the *in silico* study based on their effective cholesterol lowering activity from the existing cholesterol medications. All the parent compounds were outlined in BIOVIA discovery studio, and the structural energy of the compounds reduced up to the local minima level suing steepest plus conjugated gradient algorithm.

2.2. Novel ligand library generation

The energy minimised, and overlaid ligands were used as an input in *novel ligand generation* protocol. The maximum distance and angle threshold were set at 1.0 Å and 15° respectively for matching the ligands to produce new generations. If the distance between the atoms at each end of the bonds is greater than this value, the two bonds are not considered as matching. Generation parameter set as 3 to increase the number of combinations exponentially and usually It gives a very diverse library. BREED Algorithm is used to generate hybridised novel

Table 1
The number of new ligands generated from each basic skeleton.

Basic Ligands	No. of new ligands	Basic Ligand	No. of new ligands
Berbercine	11	6 gingerols	63
Dihydroberberine	13	Ezetimibe	31
Epiberberine	8	Stigmasterol	18
Oxyberberine	14	β-sitosterol	11
Sitosterol	12	Cholesterol	22
Stigmasterol	27	Ergosterol	32
Rosuvastatin	60	Atrovastatin	20
Pravastatin	23	Cerivastatin	19
Simvastatin	2	Comvastatin	18
Berberine methine tetrahydro group	51	Fluvastatin	37
Gemfibrozil	22	Lovastatin	1
diallyl disulphide	121	Pitavastatin	44
diallyl disulfide_8	43	Nicotinamide	26
diallyl trisulphide	83	Nicotinic Acid	27
2 vinyl 4Hi,3 dithin	3	(Pyridin − 3-yl)methanol	5
3 vinyl4h,1,2 dithin	0	1-(pyridine − 3-yl)ethan-1-one	13
Allicin	25	2-pyridin 3yl formamido ethyl nitrate	94
caffeic acid	81	Ronifibrate	38
chlorogenic acid	22	Bezafibrate	31
Cynarin	19	Ciprofibrate	39
Cynaropicrin	24	Clinofibrate	9
Scolymeside	15	Clofibrate	52
Bisabolene	62	Clofibride	9
Curcumine	30	Finofibrate	54
berberine	1		

ligands from the parent compounds, and generated ligands were converted into a library by *De novo library generation* protocol (Jafarnejad et al., 2017). The uniqueness of hybridised ligands was authenticated using public computer domains such as e - molecules, PubChem and Chemspider [supplementary].

2.3. Target receptor preparation

The crystal structure of PCSK 9 protein [PDB code: 5 OCA] was retrieved from the protein data bank (PDB) with a resolution of 2.3 Å and four chains (A, B, H, L chains) which contain 1121 residual amino acid residues (Pierce et al., 2004). Clean protein tool in DS used to correct problems due to nonstandard naming, structural disorder, protein residue connectivity, bond orders and missing side-chain or backbone atoms. It also corrects the enumeration of hydrogens according to the preferred hydrogen representation and protonation states of chain termini and *side-chains* to match the specified pH. The water molecules are removed from the protein and CHARMm (0.1 Kcal/mol) force field was applied to calculate the potential energy of the protein. Further, the coordinates are adjusted in the negative direction of the gradient, and iterative conjugate gradient minimisation algorithm is applied. Finally, the binding site of the protein was designated using define site tool, which created a sphere around the centroid of PDB ligand Dextran sulphate with the radius attuned to cover the side chains of the ligand.

2.4. Lead optimisation

In this stage ligand compound, often found in high-throughput screening hits used as starting points or scaffolds to explore more chemical space. In Discovery Studio, in situ enumeration and fragment replacement are two ways to grow a scaffold and perform scaffold hopping. This *de novo receptor* tool uses Ludi algorithm to search a library to find candidates that bind and cover the complete range of energetically favorable orientations in an active site. Structure-based in situ enumeration focuses the chemical design within the binding site of a protein target. The parameters comprised of 5 OCA and generated fragment library as input file with the radius of binding site sphere 9.714730 Å and coordinates X axis − 57.26075, Y axis 26.304837 and Z axis − 50.571616 respectively. Energy estimate-1 is used as the scoring function to prioritise the fragment hits for a receptor-based run. Maximum of 10,000 attempts to fit a fragment to a set of interaction site and density of lipophilic and polar sites set as 25 population of points. The high throughput screened hit compounds submitted for the interaction study analysis.

2.5. Docking

CHARMm-based molecular dynamics (MD) scheme was performed to dock into a PCSK9 receptor binding site. Binding site defined protein and optimised hits are given as input with centre coordinates. Then, random ligand conformations are generated using high temperature molecular dynamics under a single top hit confined to 10 random conformations of 1000 dynamic steps, and a dynamic target temperature of 1000 K. The conformations are then translated into the binding site, and final minimisation was carried to hone the ligand poses. Maximum van der Waals energy threshold was set as 300 when evaluating different ligand orientations. This protocol adds many properties to the data stream including negative of the CDOCKER energy (Gustafsen et al., 2017), negative of the CDOCKER interaction energy and Pose number of hit compound.

2.6. Structure based pharmacophore

2.6.1. Receptor ligand pharmacophore generation and ligand pharmacophore mapping

This Structure based pharmacophore studies (Wu et al., 2003) analyses and generates selective pharmacophore models grounded on receptor ligand interactions. A set of 10 receptor-based pharmacophore models for the standard ligand Dextran Sulphate was generated by *receptor – ligand pharmacophore generation* protocol in DS. Various predefined pharmacophoric features such as Hydrogen bond acceptor/donor (HBA/D), Positive ionizable/Negative ionizable (PI/NI), Hydrophobic (HY) and Ring Aromatic (RA) features were distinguished. A substantial number of pharmacophoric features were analysed to extract the desired pharmacophore model with minimum and maximum features of 4 and six respectively from the receptor binding site. After generation of the pharmacophore models, it is validated using decoy set

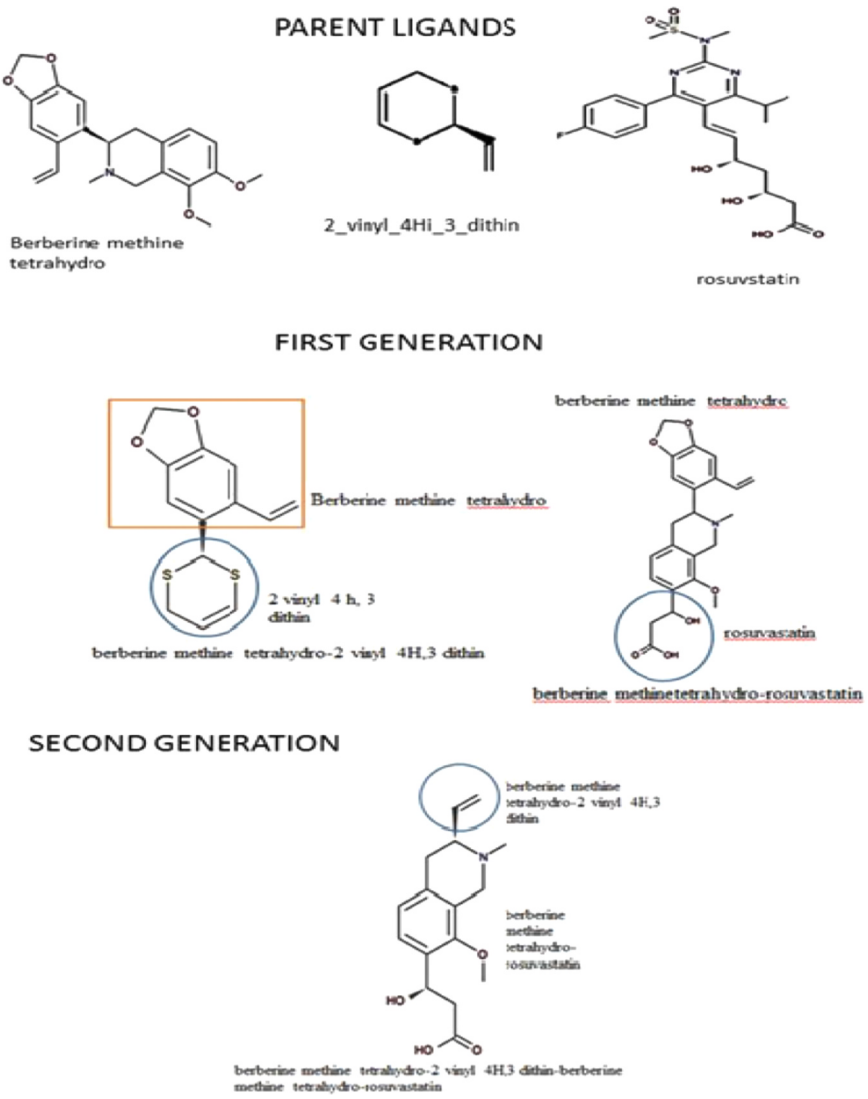

Fig. 3. Generation of one new hypercholesterolemia ligands using BREED Algorithm.

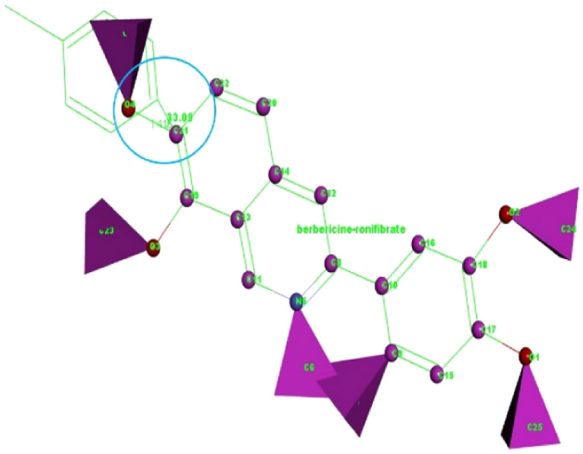

Fig. 4. Berbericine and ronifibrate mapping and hybridisation of C24 position in BREED.

(active/inactive) molecules, and receiver operating characteristic (ROC) curves are reported (Zhu et al., 2017). The best pharmacophore model was considered as a standard model to screen the hybridised hypercholesterolemia inhibitors. *Ligand Pharmacophore Mapping* protocol assists in identification and alignment of the novel hybridised ligands mapped to the generated pharmacophore model. The mapped ligands were investigated by performing all screening experiments with the BEST and Flexible Search method for analysing the mapped features. Depending on the pharmacophore, additional properties may be added; these include fit value, shape similarity and mapped atoms.

2.7. Toxicity and ADMET

The resultant compounds were subjected to toxicity and ADMET property calculation using Toxicity prediction [TOPKAT (TOxicity Prediction Komputer Assisted Technology)] protocol to prioritise promising compounds for future synthetic advancements. Significant pharmacokinetic parameters such as Ames Mutagenicity, Carcinogenic potency, Developmental toxicity potential, Skin sensitisation. Ocular and Skin Irritancy were calculated (Thangapandian et al., 2011). The ADMET (Absorption, Distribution, Metabolism, Excretion and Toxicity) Descriptors were consequently studied to eliminate the compounds with the unfavorable toxic profile. Regression model and classification models were used, and three numbers of similarity compounds are returned from the training set.

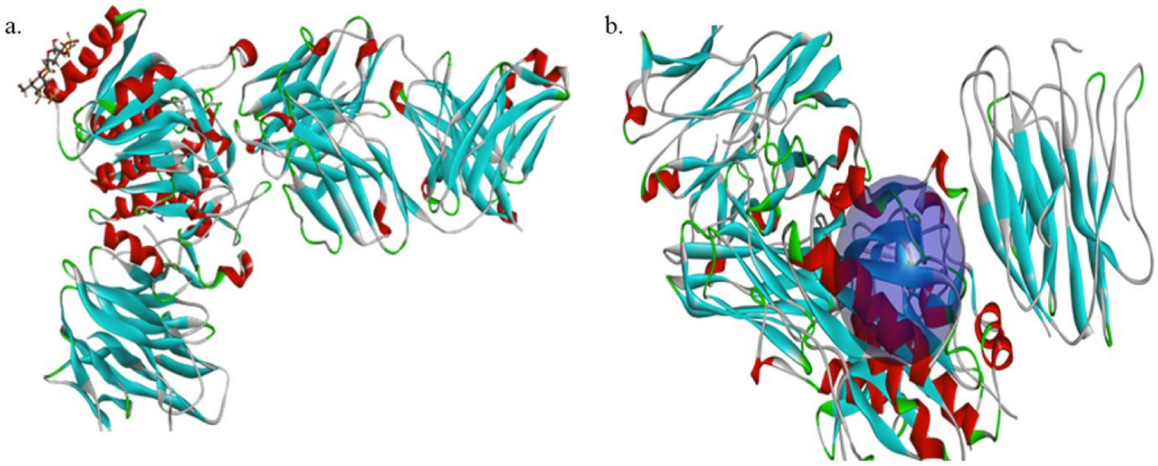

Fig. 5. a. The secondary structure of PCSK 9 protein with standard ligand Dextran Sulphate. b. The defined binding site of PCSK 9 protein.

Table 2
Minimisation report for the protein PCSK 9.

Name	FF	In.pot. Energy (kcal/mol)	Pot. Energy (kcal/mol)	vdW- Enrgy (kcal/mol)	Elect.st. energy (kcal/mol)	Int. RMS grdt.	RMS grdt.
50CA	CHARMn	− 29,662.6	− 62,956.9	− 6914.3	− 64,330.8	91.52	1.008

Note: FF- Force field; Int.pot-Initial potential; pot-potential; vdW- van der Waals; Elect. St-Electrostatic; Int. RMS. grdt-Initial Root Mean Square gradiant.

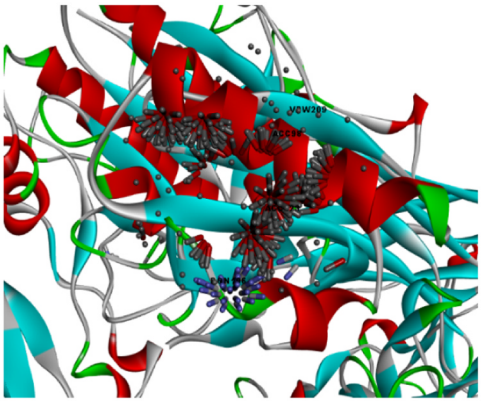

Fig. 6. Ludi interaction map of the library generated compounds with PCSK 9 protein.

2.8. Molecular dynamic simulation

Molecular dynamic (MD) simulations biologically mimic and simulate the receptor ligand complex to study the stability of interaction pattern as well as generate a realistic model of structures and analysis of time dependent structural, energetic properties. The parameters initially carry out the energy minimisation procedure using steepest descent and Adopted Basis NR methods of 1000 maximum steps followed by the heating step with a simulation time of 100 pico seconds and initial and target temperatures set as 50 and 300 K, respectively. Subsequently, Equilibration phase was carried out to ensure the distribution of appropriate energy throughout the system to achieve thermal equilibration with a simulation time of 100 pico seconds and target temperature of 300 K. The structural and energetic properties are calculated and analysed under the NPT thermodynamic ensemble of the production dynamics with a simulation time of 100 ps.

3. Results and discussion

3.1. Ligand preparation

The basic skeletons of 10 class of compounds structures were illustrated in [Fig. 1]. With the aid of these parent molecules, 51 ligands [supplementary] were chosen for design new PCSK9 inhibitors. Ligand minimisation protocol reduces the initial potential energy range of − 14.07–5599.75 kcal/mol to the local minima level − 60.03–72.05 kcal/mol [Fig. 2]. Similarly, RMS gradient also reduced to the level of 0.00488 to the 51 ligands.

3.2. Novel ligand and library generation

The results of *De novo ligand generation* protocol run produced 595 hybridised novel ligands with the aid of BREED algorithm which were formed by substitution of fragments from the parent compounds. This study generated 2 generations where the number of combinations of ligand fragments interchanged between parent molecules which resulted in a very diverse library. A total of 193 compounds were generated as first generation ligands and 244 as second-generation ligands. The Table 1 indicated number of new ligands generated from the parent 51 compounds. Fig. 3. illustrate the design of second generation molecule, berberine methane tetrahydro 2 vinyl 4 H, 3 dithin rosuvastatin by hybridisation of three parent molecule scaffolds.

Fig. 4 revealed that the matching and aligning of the berbericine and ronifibrate skeleton. BREED algorithm replaced the -H atom in the berbericine with the ronifibrates chlorobenzene group with the angle of 33° and bond distance of 1.41 Å. Searching of all the possibilities of replacements 595 ligands were generated and converted as a target library which consists of two files specifying the fragment topologies and the interaction types of fragment functional groups with (.str) and (.trg) files respectively.

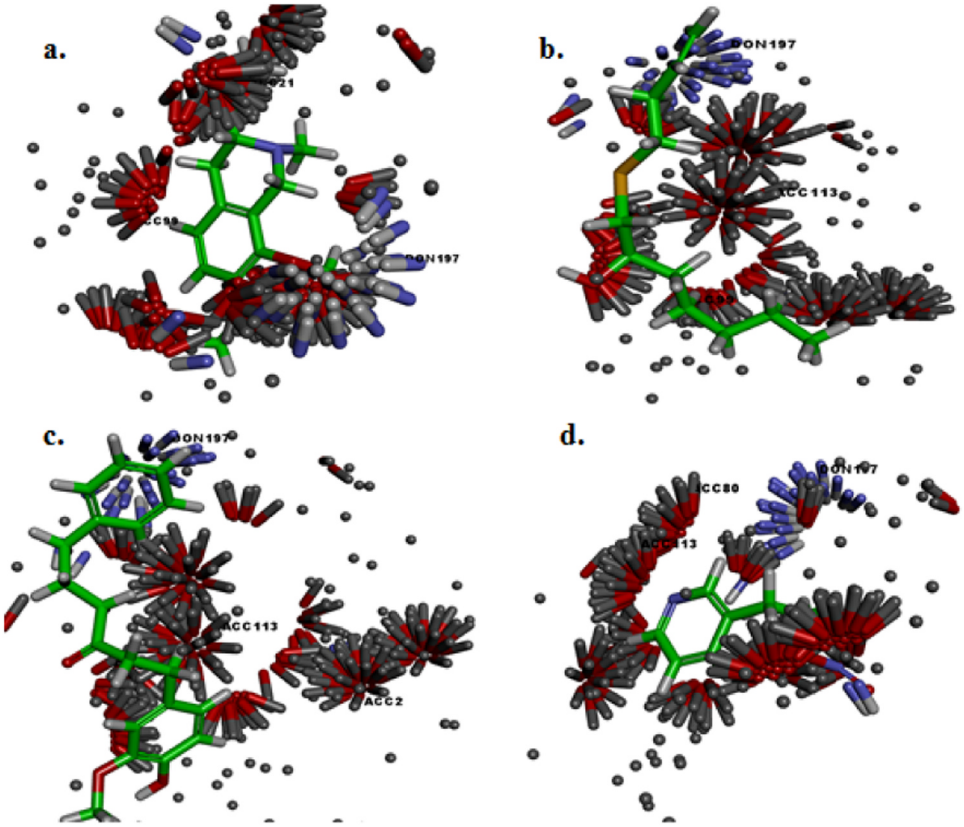

Fig. 7. Ludi interaction map with their ludi scores a. Berberine methine tetrahydro-2 vinyl 4 H, 3 dithin berberine methine tetrahydro-rosuvastatin (157), b. Diallyl disulphide-diallyl disulphide 8-diallyl disufide 8–6-gingerols, c. Nicotinamide 2-pyridin3yl formamido ethyl nitrate (120) and d. Caffeic acid-6 gingerols (77).

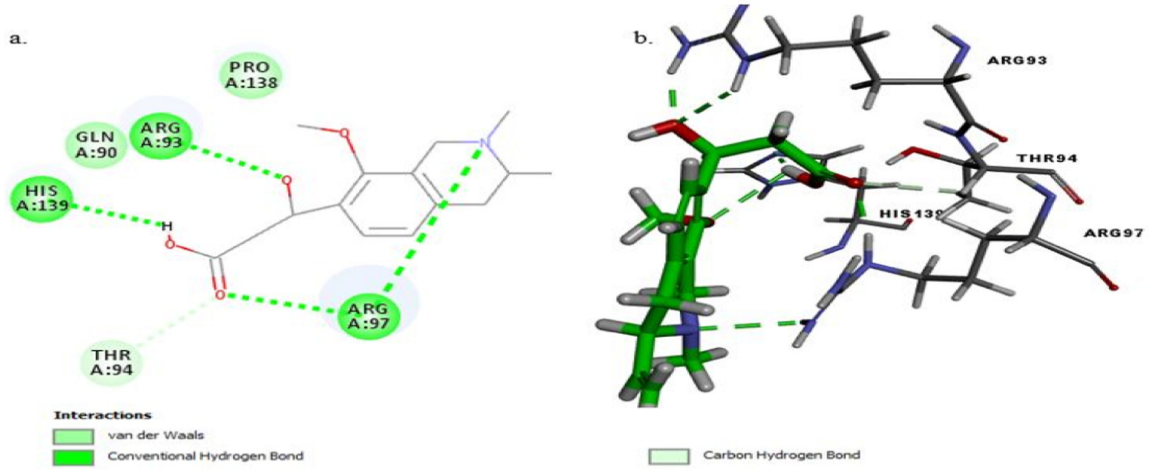

Fig. 8. a, b. 2D and 3D interaction map of the compound berberine methine tetrahydro-2 vinyl 4 H 3 dithin-berberine methine tetrahydro-rosuvastatin with the amino acid residues.

3.3. Protein preparation

PCSK 9 protein plays a vital role in the inclination of LDL levels in the blood. Hence inhibition of this protein requires urgent attention to reduce the risk of CAD. Initially, the clean report of experimental 5OCA (Fig. 5. a) corrected the 4 alternative conformation residues (E:9QZ201, D: SER72; C: SER56; B: LYS258), 3 residues backbone (B: LYS258, ARG167, ASP169) and incomplete side chains of 2 residues (C: SER56 AND D: SER72). Also, bonds and bond order of the protein was checked, and 3 terminal residues are adjusted. Eventually, the energy of the protein was reduced from an initial RMS gradient and potential energy of 91.52 Kcal/mol Å and − 29,662.6 Kcal/mol to a local minima value of 1.008 Kcal/mol Å and − 62,956.9 Kcal/mol respectively (Table 2) by the application of subsequent combination of steepest gradient and conjugate gradient algorithms. The binding site grid of the protein was projected using PDB ligand which resulted in a sphere with a radius of 9.715 Å and coordinates of X axis (57.267), Y axis (26.304), and Z axis (−50.571) (Fig. 5.b).

3.4. Lead optimisation studies

This complex and iterative stage refined the input 595 ligand structure to improve biochemical potency with selectivity to the goal of

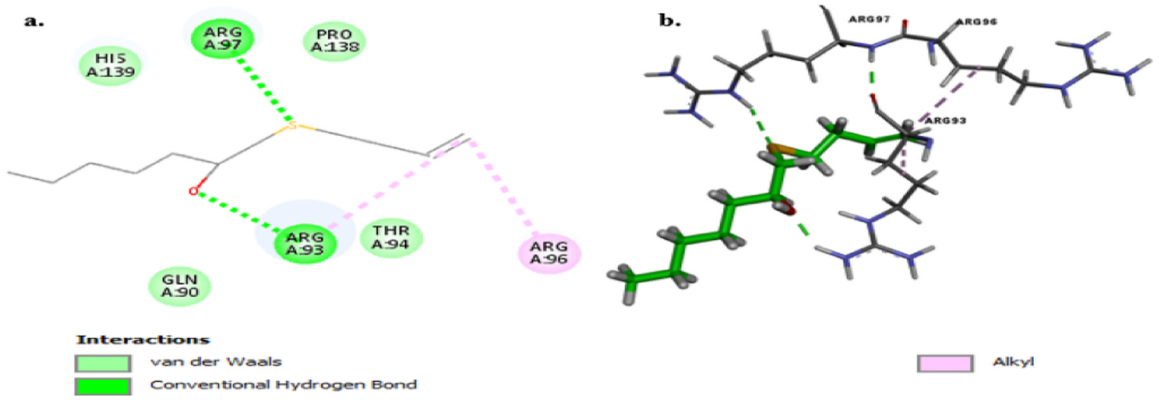

Fig. 9. a, b. 2D and 3D interaction map of the compound Diallyl disulphide 8–6-gingerols with the amino acid residues.

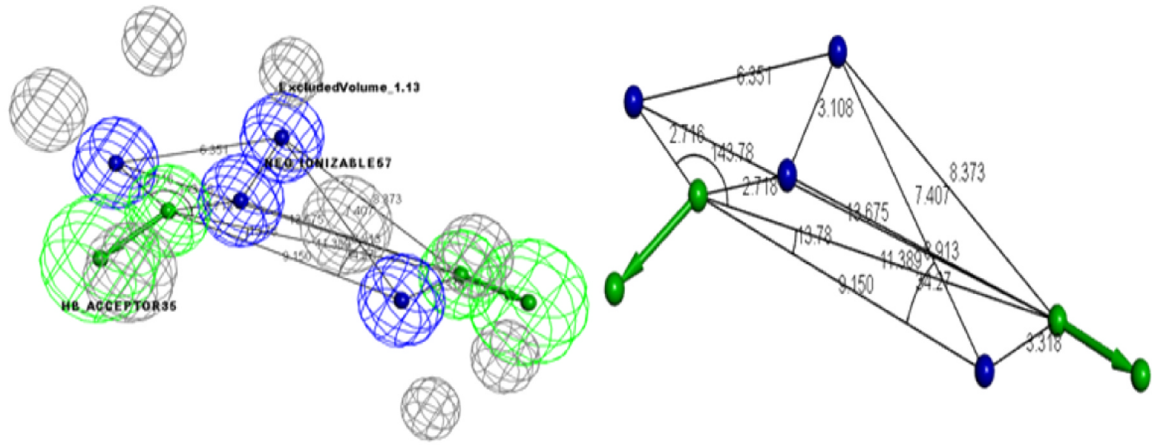

Fig. 10. Pharmacophore model 03 with distance and angles.

Table 3
Pharmacophore feature set and selectivity score of the generated Pharmacophore models.

Pharmacophore	Number of features	Feature set	Selectivity score
Pharmacophore-01	6	AANNNN	14.687
Pharmacophore-02	6	AANNNN	14.687
Pharmacophore-03	6	AANNNN	14.687
Pharmacophore-04	5	ANNNN	14.535
Pharmacophore-05	5	ANNNN	14.535
Pharmacophore-06	5	ANNNN	14.535
Pharmacophore-07	4	NNNN	14.384
Pharmacophore-08	6	AAANNN	13.159
Pharmacophore-09	6	AAANNN	13.159
Pharmacophore-10	6	AAANNN	13.159

A-Acceptor; N-Negative ionizable.

producing preclinical drug candidate. The structure-based lead optimisation focuses the chemical design with in the binding site of a protein target. The *de novo receptor* studies yielded 245 candidates that were overlaid with the generated interaction map in the active site. Fig. 6 shows the interaction map of the features of PCSK 9 active site amino acids. The fitting of the novel hybridised compounds is exhaustive allowing all combinations of interaction sites to be matched against a specific set of target sites on the scaffolds and the fragment position with the best score is saved. The compound berberine methine tetrahydro-2 vinyl 4 H, 3 dithin possessed the highest ludi score of 343, and the compound diallyl disulphide 8–6 gingerols possessed the lowest ludi score of 9. In the highest scored molecule, hydrophobic CH_3 groups mapped with negative interaction site and oxygen atom formed interaction with positive groups of the active site residues (Fig. 7a).

3.5. Interaction studies between PCSK9 and designed ligands

This grid based molecular docking method refined 245 input ligands and scored based on their interactions formed with PCSK 9 active site residues. The Fig. 8. a. showed that the best binding molecule berberine methine tetrahydro-2 vinyl 4 H 3 dithin-rosuvastatin with the Cdocker energy of −13.552 Kcal/mol. The carboxylic C=O and pyridine N atom formed 2 hydrogen bonds with Arg^{97} amino acid residue. Also, the carboxylic OH hydrogen Arg^{93} formed interactions with His ^{139}. The C=O carbonyl atom of ligand, Pro^{138}, Gln^{90} and Thr^{94} amino acid residues developed van der Waals interactions (Fig. 8b). These interactions confirm the best binding ligand compared to PDB ligand. The diallyl compound exhibits alkyl interactions with Arg^{96} (Fig. 9). The gingerol group containing ligand specially reveals its pi-cationic interactions with Arg^{93} amino acid. The niacin class of compounds forms an unfavorable bond with Arg^{93} amino acid. So it possesses the less Cdocker energy of −11.1763 Kcal/mol.

3.6. Structure based pharmacophore

3.6.1. Receptor ligand pharmacophore and ligand pharmacophore mapping

A set of selective pharmacophore models were identified from the interaction between the PDB ligand-protein (5OCA) complexes. This protocol enumerates acceptor and negative pharmacophore features from the PDB ligand was match the receptor-ligand interaction. The binding interaction. Excluded volumes are placed around the residues atoms at 1.5–5.0 Å from the ligand. A number of pharmacophore models were generated and retained the best 10 most selective pharmacophores. The best pharmacophore model was selected based on the nature of pharmacophoric features, a number of features and the

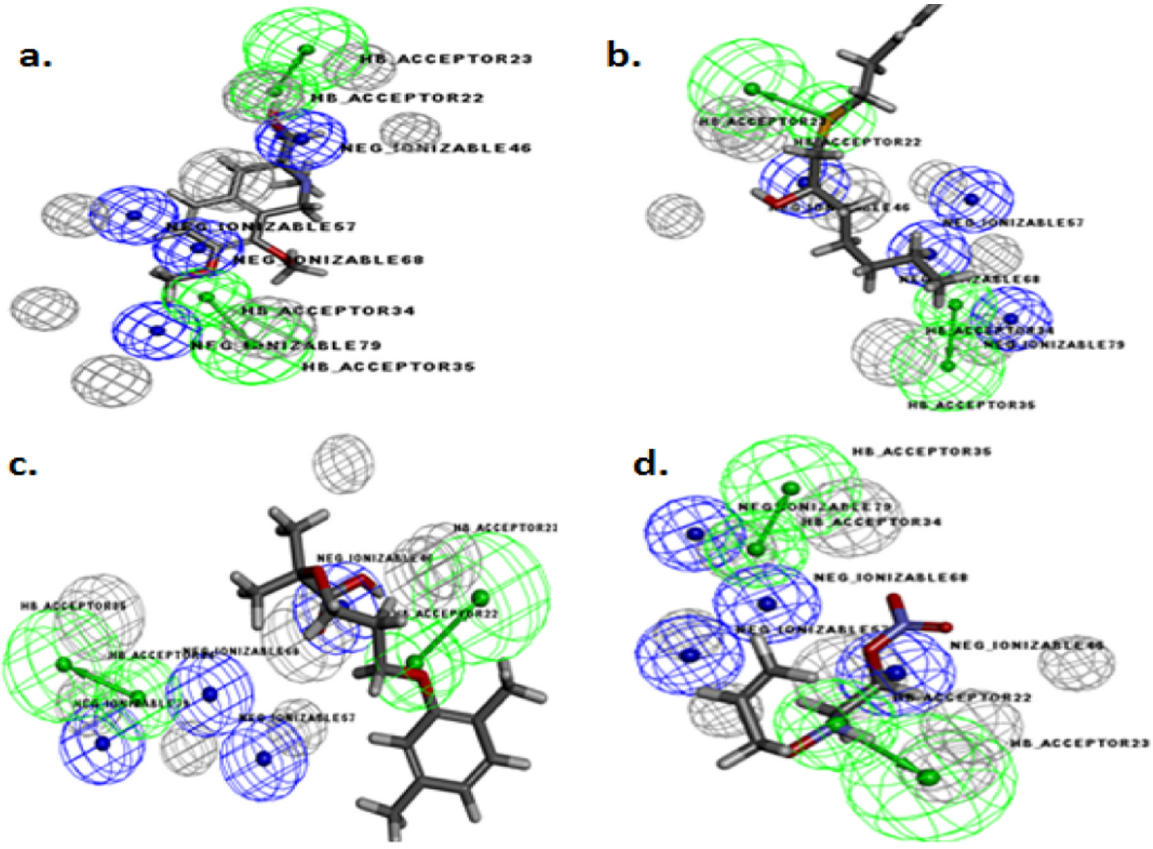

Fig. 11. Ligand pharmacophore mapping of the compounds a.) Berberine methine teetrahydro-2 vinyl 4 H 3 dithin-berberine methane tetrahydro-rosuvastatin, b.) Diallyl disulphide-diallyl disulphide 8-diallyl disufide 8–6-gingerols, c.) Caffeic acid-6 gingerols, d.)2-pyridin3yl formamido ethyl nitrate-ciprofibrate-diallyl_disulfide- ciprofibrate.

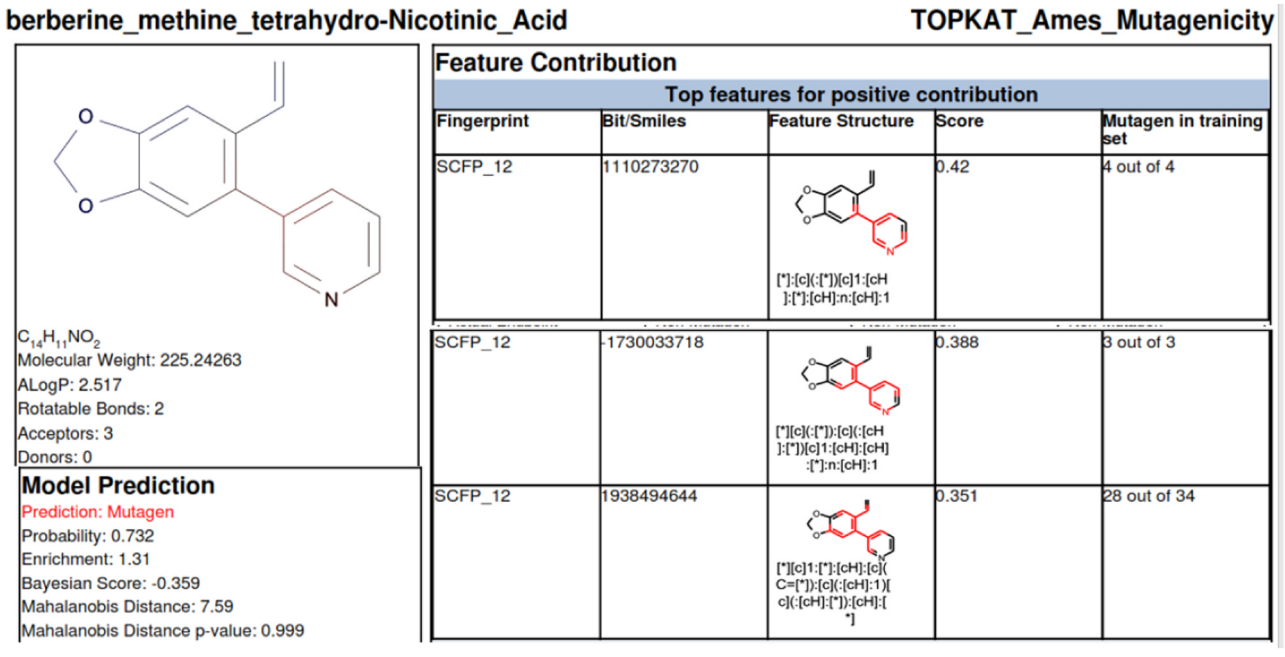

Fig. 12. Mutagenicity prediction of one of the berberine derivative.

Table 4
ADMET properties selected compounds.

Compound	Solubility*	Absorption**	Hepatotoxic	PPB	BBB***
Compound 2	4	0	false	false	3
Compound 3	3	0	false	false	3
Compound 5	5	0	false	false	3
Compound 6	4	0	false	false	2
Compound 15	3	0	false	false	2
Compound 16	3	0	false	false	2
Compound 20	3	0	false	false	3
Compound 58	2	0	false	false	1
Compound 59	2	0	false	false	1
Compound 75	3	0	false	false	1
Compound 76	3	0	false	false	2
Compound 72	3	0	false	false	3
Compound 73	3	0	false	false	3
Compound 81	3	0	false	false	3
Compound 90	3	0	false	false	3

* 0-extremely low; 1-Very low; 2-Low; 3-Good; 4-Optimal.
** 0-good; 1-Moderate; 2-Poor; 3-Very poor.
*** 0-Very high penetrant; 1-High; 2-Medium; 3-Low; 4 – Undefined.

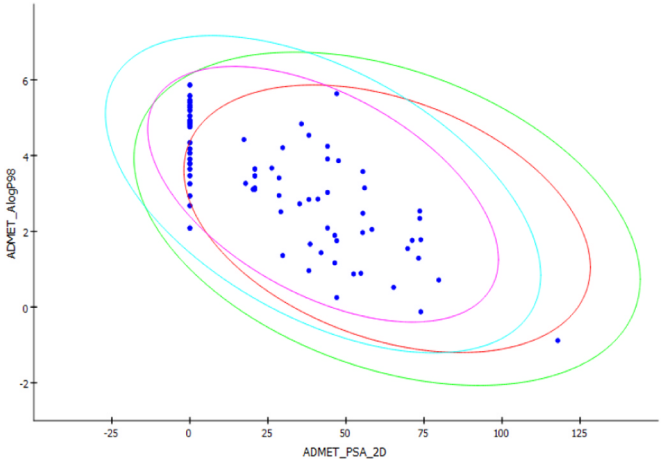

Fig. 13. Absorption measurement plot.

selectivity score as well as decoy set validation. Among the ten pharmacophores generated, pharmacophore- 03 model was selected based on the distance, angle between the various pharmacophoric features and predictive power.

Fig. 10 revealed that the pharmacophore model 03 contains two acceptors and four negative features with the selectivity score of 14.687 (Table 3). The distance between the two acceptors is 11.38 Å, and negative ionizable feature ranges from 3.1 to 13.67 Å.

The best pharmacophore model 03 was used as standard query model to identify the best binding ligands (245 docked), that maps to a pharmacophore and aligns to the query. This protocol calculated features, shapes, and excluded volume of the ligands. Additionally, it added the fit value, shape similarity, and atom maps. The fit value for the ligands ranges between 0.9938 and 2.9985. Among the 245 ligands, 96 ligands were mapped well to the features of pharmacophore 3. The Fig. 11 demonstrates the best mapping ligands of four classes.

3.7. Toxicity prediction

TOPKAT rapidly and precisely assessed the ability of the molecule to reach a site and the ability of the molecule to chemically interact with the biological system of the site to produce a toxic response. Robust, cross-validated, rich descriptor containing Quantitative Structure-Toxicity Relationship (QSTR) models predict the specific toxicological endpoints of 96 hit molecules from the docking result. All query molecules are checked for substructure and comparing all 1 and 2 atom fragments from the modeled training set (Fig. 12). Among the 96 molecules 48 molecules descriptor falling out of the range in training set, it indicated that the 48-query structure outside the model applicability. The analysed and interpreted results revealed that 48 ligands were free of toxicity profile. The Fig. 12 explained that the one of the second generation berberine derivative fragment mapped with the standard toxic training set compounds. Hence the compound predicted as a mutagenic profile.

3.8. ADMET studies

The generated novel ligands have better cholesterol reducing drug-like properties than the parent berberine. The active constituents that contribute the pharmacological activity are necessarily orally and antilipidemic active, i.e., the compound must be absorbed through the intestine and penetrate the BBB. Numerous article revisions acknowledged the criteria for cholesterol reducing drug properties that have been found to include molecular weight < 490, polar surface area (PSA) < 70–90 Å2 (upper limit is 90 Å2), Log P < 5, H-bond donor < 4, H-bond acceptor < 6 and number of rotatable bonds < 7 (Pirhadi and Ghasemi, 2012; Susnow and Dixon, 2003). From Table 4, among 48 hit molecules, 28 compounds fail to meet some of the criteria such as log P, MW and hepatotoxicity profile. In particular, the berberine moieties reduces the hydrogen-bonding capacity and molecular flexibility and increases the lipophilicity of the molecule compared to the other molecules (Meyer et al., 1996). The human intestinal absorption (HIA) and BBB penetration model of ADMET are defined by 95% and 99% confidence ellipses in the ADMET_PSA_2D plot (Fig. 13) (Egan and Lauri, 2002). These ellipses describe the areas of compounds that are well-absorbed and capable of penetrating the BBB are expected to be found. Compounds outside the 95% and 99% significant ellipsoids are considered to possess very low intestinal absorption and BBB penetration (Balasubramaniyan et al., 2018). Out of the 48 ligands, 15 ligands (Table 5) were found to be satisfactory concerning absorption, solubility, BBB, PPB and hepatotoxicity.

3.9. Molecular dynamic simulation

Molecular dynamics (MD) simulation is a potentially influential tool for understanding the structural, dynamic, and functional characteristics of proteins at an atomic level of detail. To endorse the results of high-ranking ligand from the molecular docking CDOCKER, dynamic simulation studies have been carried out for further evaluation of stability of PCSK 9 and inhibitor complex. The results from dynamic studies generated a realistic model of a PCSK 9 protein structure motion, conformation, produce a time sequence analysis of conformational and energetic properties, explore energy decay, and a solvent effect. After the two energy minimisation steps in the essence of the molecular dynamics technique, the experimental crystal structure (5OCA) PCSK 9 with PDB ligand (dextran sulphate) reached the potential energy of −21,837.470 kcal/mol and RMS gradient of 0.079 kcal/molÅ. Similarly, the docked complex reached the final potential energy of −64,276.216 kcal/mol and RMS gradient of 0.098 kcal/molÅ. The heating step prepared the molecular system to reach ideal temperature for further process. At the end of equilibration step, both the complex became stable at 200–225 ps. In this state, the initial and final RMS gradients for standard dextran sulphate (PDB) was of 18.851 and 19.173 kcal/ molÅ and 19.196 and 19.572 kcal/molÅ (Table 6) for the

docked berberine derivative-protein complex. Energy terms of the production run showed that the PCSK 9 receptor and inhibitor complex attained stable state at 192 ps (Fig. 14) with a total energy of −47,000 Kcal/mol.

3.10. Analysis of trajectories and residual impact

The Trajectory analysis of stable complex obtained from production stage described the 100 conformational behavior and effect of the designed ligand on residues of the active sites. There is no RMSD value variation between the PDB complex and lead ligand complex confirmations. Similarly, there is no root mean square fluctuations (Fig. 15. a) between both the complex except residues of 382–560 (Fig. 15.b) in the ligand complex. These fluctuations indicated that the lead compound denatured the PCSK9 receptor. It leads to inhibition of PCSK9, which indirectly paves the way for a reduction in blood LDL cholesterol levels.

Table 5
Final 15 compounds along with their IUPAC name and molecular weight.

Compound	Structure	IUPAC name	MW in grams
2	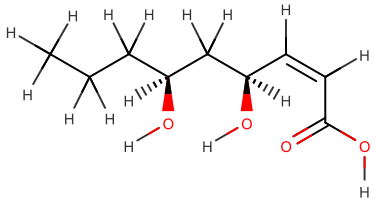	(2Z,4S,6S)-4,6-dihydroxynon-2-enoic acid	188.223
3	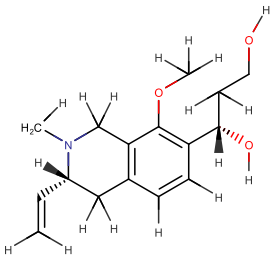	(3S)-3-[(3R)-3-ethenyl-8-methoxy-2-methyl-1,2,3,4-tetrahydroisoquinolin-7-yl]-3-hydroxypropanoic acid	291.347
5	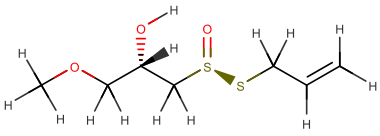	(2S)-1-methoxy-3-[(S)-(prop-2-en-1-ylsulfanyl)sulfinyl]propan-2-ol	210.31
6	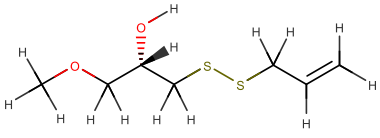	(2S)-1-methoxy-3-(prop-2-en-1-yldisulfanyl)propan-2-Ol	194.31

(continued on next page)

Table 5 (*continued*)

15	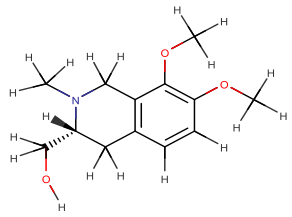	[(3R)-7,8-dimethoxy-2-methyl-1,2,3,4-tetrahydroisoquinolin-3-yl]methanol	237.299
16	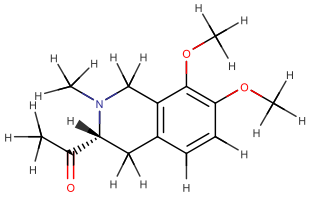	1-[(3R)-7,8-dimethoxy-2-methyl-1,2,3,4-tetrahydroisoquinolin-3-yl]ethan-1-one	249.310
58	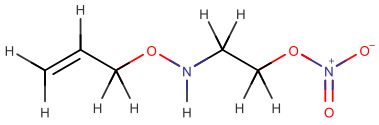	2-[(prop-2-en-1-yloxy)amino]ethyl nitrate	162.145
59	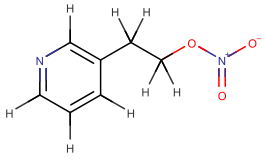	2-(pyridin-3-yl)ethyl nitrate	168.152
75	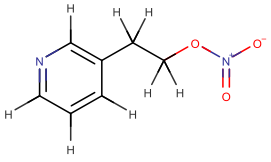	2-phenylethoxy hydrogen carbonate	182.175
76	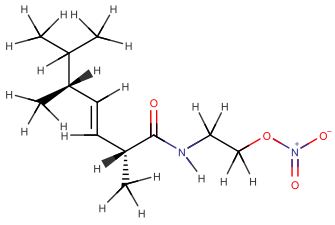	(2R,3E,5R)-2,5,6-trimethyl-N-[2-(nitrooxy)ethyl]hept-3-enamide	258.318

(*continued on next page*)

Table 5 (*continued*)

72	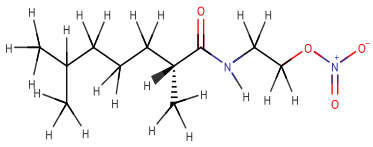	(2R)-2,6-dimethyl-N-[2-(nitrooxy)ethyl]heptanamide	246.307
73	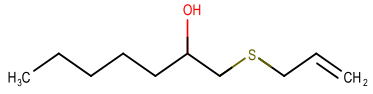	1-(prop-2-en-1-ylsulfanyl)heptan-2-ol	188.33
20	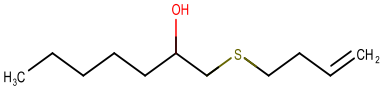	1-(but-3-en-1-ylsulfanyl)heptan-2-ol	202.36
81	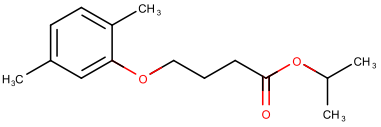	propan-2-yl 4-(2,5-dimethylphenoxy)butanoate	250.338
90	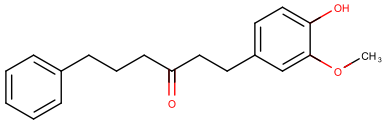	1-(4-hydroxy-3-methoxyphenyl)-6-phenylhexan-3-one	298.382

Table 6
Molecular Dynamic simulation table.

Name	Stage	I.P. (Kcal/mol)	T.E (Kcal/mol)	P.E (Kcal/mol)	K.E (Kcal/mol)	TEM (k)	V.W.E Kcal/mol	E.S.E Kcal/mol	I.RMS.G Kcal/molÅ	F.RMS.G Kcal/(molÅ
PCSK 9 with Standard Ligand Dextran Sulphate										
5OCA	MMN	−7105.83		−16,999.80			−7725.77	−13,392.06	91.45	0.91
5OCA	MMN	−16,999.80		−21,837.47			−8073.43	−17,969.87	0.91	0.08
5OCA	HTG	−21,837.47	−1205.47	−12,790.03	11,584.56	309.08	−7121.47	−19,951.13	1.92	18.85
5OCA	EQN	−12,790.02	−1200.04	−12,882.32	11,682.28	309.67	−7303.53	−20,074.70	18.85	19.17
5OCA	PDN	−12,882.32	−2205.74	−13,571.88	1136.614	301.29	−7289.38	−20,323.67	19.17	18.71
PCSK 9 with designed ligand complex										
50CA	MMN	−57,685.96		−16,999.80			−7725.77	−13,392.06	91.45	0.91
5OCA	MMN	−59,233.52		−21,837.47			−8073.43	−17,969.87	0.90	0.08
5OCA	HTG	−64,276.21		−12,790.02	11,395.19	302.43	−6036.32	−65,164.98	3.75	19.91
5OCA	EQN	−54,160.95	−42,765.75	−12,882.32	11,613.04	308.21	−6033.55	−69,917.44	19.19	18.57
5OCA	PDN	−58,253.32	−46,640.28	−13,571.88	11,203.54	297.34	−6085.71	−70,118.78	19.57	19.32

I.P. E – Initial Potential Energy, T. E – Total Energy, P. E – Potential Energy, K. E – Kinetic Energy, TEMP – Temperature, V. W. E – Vander Waals Energy, E. S. E – Electrostatic Energy, I. RMS. G – Initial RMS Gradient, F. RMS. G – Final RMS Gradient, MMN – Minimisation, HTG – Heating, EQN – Equilibration, PDN – Production.

4. Conclusion

In this study, various computational methodologies like lead optimisation, docking, structure-based pharmacophore, toxicity, ADMET (Absorption, Distribution, Metabolism, Excretion and Toxicity) and molecular dynamic simulation studies were used to identify potent and safe lead ligands for the target PCSK-9. At the end of the studies, 15 lead molecules are proved to be as potent and safe PCSK9 inhibitors, and it can serve as a feasible treatment for CAD with less toxic effects. Computationally, it has been found that the lead molecules exhibited comparatively higher activity than the standard ligand Dextran Sulphate. It has also been found that the identified lead molecules have

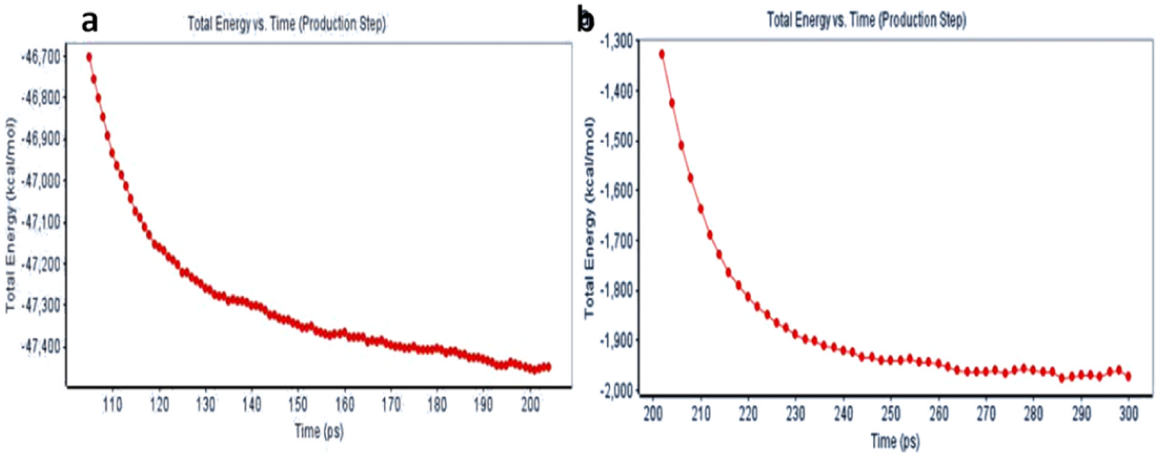

Fig. 14. Dynamic production run a).Simulation time (ps) Vs total energy (kcal/mol) of PDB complex b). Simulation time (ps) Vs Temperature (k) change of PDB complex and docked berberine derivative complex.

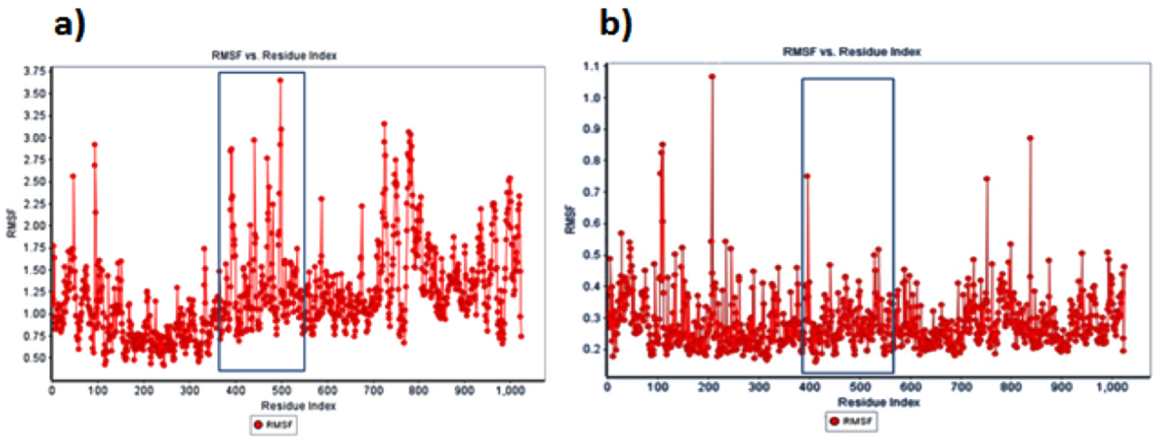

Fig. 15. Trajectory analysis a) RMSF of PDB complex b) RMSF of berberine derivative docked with protein.

not been reported yet and is undeniably novel.

Conflicts of interest

There are no conflicts to declare References

Funding Sources

There is no funding sources supported to this study.

Appendix A. Supplementary material

Supplementary data associated with this article can be found in the online version at doi:10.1016/j.bcab.2018.12.014.

References

Abumweis, S., Barake, R., Jones, P., 2008. Plant sterols/stanols as cholesterol lowering agents: a meta-analysis of randomized controlled trials. Food Nutr. Res. 52, 1811. https://doi.org/10.3402/fnr.v52i0.1811.

Pierce, *, Albert C., Rao, Govinda, Bemis, G.W., 2004. BREED: generating Novel Inhibitors through Hybridization of Known Ligands. Appl. CDK2, P38, HIV Protease. https://doi.org/10.1021/JM030543U.

Balasubramaniyan, S., Irfan, N., Umamaheswari, A., Puratchikody, A., 2018. Design and virtual screening of novel fluoroquinolone analogs as effective mutant DNA GyrA inhibitors against urinary tract infection-causing fluoroquinolone resistant *Escherichia coli*. RSC Adv. 8, 23629–23647. https://doi.org/10.1039/C8RA01854E.

Corzomartinez, M., Corzo, N., Villamiel, M., 2007. Biological properties of onions and garlic. Trends Food Sci. Technol. 18, 609–625. https://doi.org/10.1016/j.tifs.2007.07.011.

Egan, W.J., Lauri, G., 2002. Prediction of intestinal permeability. Adv. Drug Deliv. Rev. 54, 273–289.

Farmer, J.A., 2009. Nicotinic acid: a new look at an old drug. Curr. Atheroscler. Rep. 11, 87–92.

Farnier, M., 2014. PCSK9: from discovery to therapeutic applications. Arch. Cardiovasc. Dis. 107, 58–66. https://doi.org/10.1016/j.acvd.2013.10.007.

Gustafsen, C., Olsen, D., Vilstrup, J., Lund, S., Reinhardt, A., Wellner, N., Larsen, T., Andersen, C.B.F., Weyer, K., Li, J.-P, Seeberger, P.H., Thirup, S., Madsen, P., Glerup, S., 2017. Heparan sulfate proteoglycans present PCSK9 to the LDL receptor. Nat. Commun. 8, 503. https://doi.org/10.1038/s41467-017-00568-7.

Jafarnejad, S., Keshavarz, S.A., Mahbubi, S., Saremi, S., Arab, A., Abbasi, S., Djafarian, K., 2017. Effect of ginger (Zingiber officinale) on blood glucose and lipid concentrations in diabetic and hyperlipidemic subjects: a meta-analysis of randomized controlled trials. J. Funct. Foods 29, 127–134. https://doi.org/10.1016/j.jff.2016.12.006.

Willerson, James T., Holmes, David R., 2004. Coronary Artery Disease. Springerhttps://doi.org/10.1007/978-1-4471-2828-1.

Khera, A.V., Qamar, A., Reilly, M.P., Dunbar, R.L., Rader, D.J., 2015. Effects of niacin, statin, and fenofibrate on circulating proprotein convertase subtilisin/kexin type 9 levels in patients with dyslipidemia. Am. J. Cardiol. 115, 178–182. https://doi.org/10.1016/j.amjcard.2014.10.018.

Krishnan, M.N., 2012. Coronary heart disease and risk factors in India - on the brink of an epidemic? Indian Heart J. 64, 364–367. https://doi.org/10.1016/j.ihj.2012.07.001.

Li, L., Zhou, X., Li, N., Sun, M., Lv, J., Xu, Z., 2015. Herbal drugs against cardiovascular disease: traditional medicine and modern development. Drug Discov. Today 20, 1074–1086. https://doi.org/10.1016/j.drudis.2015.04.009.

Maji, D., Shaikh, S., Solanki, D., Gaurav, K., 2013. Safety of statins. Indian J. Endocrinol. Metab. 17, 636–646. https://doi.org/10.4103/2230-8210.113754.

Mendis, S., Puska, P., Norrving, B., 2011. World Health Organization., World Heart Federation., World Stroke Organization. Global atlas on cardiovascular disease prevention and control. World Health Organization in collaboration with the World Heart Federation and the World Stroke Organization.

Meyer, M., Wilson, P., Schomburg, D., 1996. Hydrogn bonding and molecular shape complementray as a basis for protein docking. J. Mol. Biol. 264, 199–210.

Momtazi, A.A., Banach, M., Pirro, M., Katsiki, N., Sahebkar, A., 2017. Regulation of PCSK9 by nutraceuticals. Pharmacol. Res. 120, 157–169. https://doi.org/10.1016/j.

phrs.2017.03.023.
Natarajan, P., Kathiresan, S., 2016. PCSK9 inhibitors. Cell 165, 1037. https://doi.org/10.1016/j.cell.2016.05.016.
Pirhadi, S., Ghasemi, J.B., 2012. Pharmacophore identification, molecular docking, virtual screening, and in silico ADME studies of non-nucleoside reverse transcriptase inhibitors. Mol. Inform. 31, 856–866. https://doi.org/10.1002/minf.201200018.
Rallidis, L.S., Lekakis, J., 2016. PCSK9 inhibition as an emerging lipid lowering therapy: unanswered questions. Hell. J. Cardiol. 57, 86–91. https://doi.org/10.1016/j.hjc.2016.03.002.
Rao, M., Xavier, D., Devi, P., Sigamani, A., Faruqui, A., Gupta, R., Kerkar, P., Jain, R.K., Joshi, R., Chidambaram, N., Rao, D.S., Thanikachalam, S., Iyengar, S.S., Verghese, K., Mohan, V., Pais, P., 2015. Prevalence, treatments and outcomes of coronary artery disease in Indians: a systematic review. Indian Heart J. 67, 302–310. https://doi.org/10.1016/j.ihj.2015.05.003.
Ried, K., 2016. Garlic lowers blood pressure in hypertensive individuals, regulates serum cholesterol, and stimulates immunity: an updated meta-analysis and review. J. Nutr. 146, 389S–396S. https://doi.org/10.3945/jn.114.202192.
Robinson, J.G., Farnier, M., Krempf, M., Bergeron, J., Luc, G., Averna, M., Stroes, E.S., Langslet, G., Raal, F.J., El Shahawy, M., Koren, M.J., Lepor, N.E., Lorenzato, C., Pordy, R., Chaudhari, U., Kastelein, J.J.P., 2015. Efficacy and safety of alirocumab in reducing lipids and cardiovascular events. N. Engl. J. Med. 372, 1489–1499. https://doi.org/10.1056/NEJMoa1501031.
Rubins, H.B., Robins, S.J., Collins, D., Fye, C.L., Anderson, J.W., Elam, M.B., Faas, F.H., Linares, E., Schaefer, E.J., Schectman, G., Wilt, T.J., Wittes, J., 1999. Gemfibrozil for the secondary prevention of coronary heart disease in men with low levels of high-density lipoprotein cholesterol. N. Engl. J. Med. 341, 410–418. https://doi.org/10.1056/NEJM199908053410604.
Sabatine, M.S., Giugliano, R.P., Keech, A.C., Honarpour, N., Wiviott, S.D., Murphy, S.A., Kuder, J.F., Wang, H., Liu, T., Wasserman, S.M., Sever, P.S., Pedersen, T.R., 2017. Evolocumab and clinical outcomes in patients with cardiovascular disease. N. Engl. J. Med. 376, 1713–1722. https://doi.org/10.1056/NEJMoa1615664.
Singh, I.P., Mahajan, S., 2013. Berberine and its derivatives: a patent review (2009 – 2012). Expert Opin. Ther. Pat. 23, 215–231. https://doi.org/10.1517/13543776.2013.746314.
Steinberg, D., Witztum, J.L., 2009. Inhibition of PCSK9: a powerful weapon for achieving ideal LDL cholesterol levels. Proc. Natl. Acad. Sci. USA 106, 9546–9547. https://doi.org/10.1073/pnas.0904560106.
Susnow, R.G., Dixon, S.L., 2003. Use of robust classification techniques for the prediction of human cytochrome P450 2D6 inhibition. J. Chem. Inf. Comput. Sci. 43, 1308–1315. https://doi.org/10.1021/ci030283p.
Thangapandian, S., John, S., Lee, Y., Kim, S., Lee, K.W., 2011. Dynamic structure-based pharmacophore model development: a new and effective addition in the histone Deacetylase 8 (HDAC8) inhibitor discovery. Int. J. Mol. Sci. 12, 9440–9462. https://doi.org/10.3390/ijms12129440.
WHO | Disease burden and mortality estimates, 2018a. WHO.
WHO | Disease burden and mortality estimates, 2018b. WHO.
WHO | Global atlas on cardiovascular disease prevention and control, 2015. WHO.
Wongbutdee, J., 2009. Physiological effects of Berberine. Thai Pharm. Heal. Sci. J. 4.
Wu, G., Robertson, D.H., Brooks, C.L., Vieth, M., 2003. Detailed analysis of grid-based molecular docking: a case study of CDOCKER? A CHARMm-based MD docking algorithm. J. Comput. Chem. 24, 1549–1562. https://doi.org/10.1002/jcc.10306.
Zhu, X., Zhou, L., Zhong, L., Dai, D., Hong, M., You, R., Wang, T., 2017. Molecular Simulation Exploration of potential RSK2 inhibitors by pharmacophore modelling, structure-based 3D- QSAR, molecular docking study and molecular dynamics simulation Exploration of potential RSK2 inhibitors by pharmacophore modelling, structure- based 3D-QSAR, molecular docking study and molecular dynamics simulation. Mol. Simul. 43, 534–547. https://doi.org/10.1080/08927022.2016.1274987.